Diapir structure and its constraint on gas hydrate accumulation in the Makran accretionary prism, offshore Pakistan

Zhen Zhang, Gao-wen He, Hui-qiang Yao, Xi-guang Deng, Miao Yu, Wei Huang, Wei Deng, Syed Waseem Haider, Naimatullah Sohoo, Noor Ahmed Kalhoro

Citation: Zhen Zhang, Gao-wen He, Hui-qiang Yao, Xi-guang Deng, Miao Yu, Wei Huang, Wei Deng, Syed Waseem Haider, Naimatullah Sohoo, Noor Ahmed Kalhoro, 2020. Diapir structure and its constraint on gas hydrate accumulation in the Makran accretionary prism, offshore Pakistan, China Geology, 3, 611-622. doi: 10.31035/cg2020049.

View online: https://doi.org/10.31035/cg2020049

China Geology 4 (2020) 611−622

China Geology

Journal homepage: http://chinageology.cgs.cn
https://www.sciencedirect.com/journal/china-geology

Diapir structure and its constraint on gas hydrate accumulation in the Makran accretionary prism, offshore Pakistan

Zhen Zhang[a, b,*], Gao-wen He[a, b], Hui-qiang Yao[a, b], Xi-guang Deng[a, b], Miao Yu[a, b], Wei Huang[a], Wei Deng[a], Syed Waseem Haider[c], Naimatullah Sohoo[c], Noor Ahmed Kalhoro[c]

[a] *Ministry of Natural Resources Key Laboratory of Marine Mineral Resources, Guangzhou Marine Geological Survey, China Geological Survey, Ministry of Natural Resources, Guangzhou* 510760, *China*

[b] *Southern Marine Science and Engineering Guangdong Laboratory (Guangzhou), Guangzhou* 511458, *China*

[c] *National Institute of Oceanography, Karachi* 75600, *Pakistan*

ARTICLE INFO

Article history:
Received 17 May 2020
Received in revised form 29 May 2020
Accepted 19 June 2020
Available online 25 August 2020

Keywords:
Natural gas hydrate
Mud diapir
Mud volcano
Gas chimney
Makran accretionary prism
Marine geological survey engineering
Offshore Pakistan

ABSTRACT

The Makran accretionary prism is located at the junction of the Eurasian Plate, Arabian Plate and Indian Plate and is rich in natural gas hydrate (NGH) resources. It consists of a narrow continental shelf, a broad continental slope, and a deformation front. The continental slope can be further divided into the upper slope, middle slope, and lower slope. There are three types of diapir structure in the accretionary prism, namely mud diapir, mud volcano, and gas chimney. (1) The mud diapirs can be grouped into two types, namely the ones with low arching amplitude and weak-medium activity energy and the ones with high arching amplitude and medium-strong activity energy. The mud diapirs increase from offshore areas towards onshore areas in general, while the ones favorable for the formation of NGH are mainly distributed on the middle slope in the central and western parts of the accretionary prism. (2) The mud volcanoes are mainly concentrated along the anticline ridges in the southern part of the lower slope and the deformation front. (3) The gas chimneys can be grouped into three types, which are located in piggyback basins, active anticline ridges, and inactive anticline ridges, respectively. They are mainly distributed on the middle slope in the central and western parts of the accretionary prism and most of them are accompanied with thrust faults. The gas chimneys located at different tectonic locations started to be active at different time and pierced different horizons. The mud diapirs, mud volcanoes, and gas chimneys and thrust faults serve as the main pathways of gas migration, and thus are the important factors that control the formation, accumulation, and distribution of NGH in the Makran accretionary prism. Mud diapir/gas chimney type hydrate develop in the middle slope, mud volcano type hydrate develop in the southern lower slope and the deformation front, and stepped accretionary prism type hydrate develop on the central and northern lower slope. The middle slope, lower slope and deformation front in the central and western parts of the Makran accretionary prism jointly constitute the NGH prospect area.

1. Introduction

The Makran accretionary prism located in the northern part of the Arabian Sea is the largest accretionary prisms in the world (Gutscher MA and Westbrook GK, 2009). It has attracted extensive attention with its unique tectonic location and rich NGH resources. Since the 1980s, scientific research institutions from many countries led by Germany have carried out geological and geophysical survey and research related to NGH in Makran (von Rad U et al., 2000; Kukowski N et al., 2001; Bohrmann G et al., 2008; Römer M et al., 2012), discovering great numbers of diapir structure of various types from seismic profiles and multi-beam topographic maps. Diapir structure, as a special form of upward migration of fluid in deep sources (He JX et al., 2019), are present in the forms of mud diapirs, mud volcanoes, gas chimneys and seafloor pockmarks, which represent different evolutionary stages of fluid and low-density rocks, namely plastic arching, piercing, and collapse, respectively (He JX et al., 1994; Dong WL and Huang BJ, 2000; Shi WZ et al., 2009). Therefore,

* Corresponding author: *E-mail address*: zhangzhenhnpy@163.com (Zhen Zhang).

doi:10.31035/cg2020049
2096-5192/© 2020 China Geology Editorial Office.

these structures serve as important window for the understanding of the deep fluid activities.

The Makran accretionary prism, offshore Pakistan is a natural laboratory for the study of mud diapirs, mud volcanoes, and gas chimneys owing to its thick incoming sediments (Kopp C et al., 2000; Grando G and McClay K, 2007), inverted formation density, high deposition rate (Abid H et al., 2015), and regional strike-slip fault system (Platt JP et al., 1988; Grando G and McClay K, 2007). Minshull TA and White R (1989) and Schlüter HU et al. (2002) discovered mud volcanoes along the Makran coast and argued that they were formed as the water filled with gas escaped to the earth surface. Grando G and McClay K (2007) found that spectacular mud diapirs and mud volcanoes existed inside the accretionary prism, with most mud volcanoes being distributed along thrust anticlines and Bottom Simulating Reflectors (BSRs) developing on the top of some mud diapirs. As indicated by the study on four mud volcanoes along the Makran coast in southeast Iran conducted by Babadi MF et al. (2019), the mud volcano system makes an important contribution to fluid migration. However, in-depth research is yet to be conducted for the systematical understanding of the mud diapirs, mud volcanoes, and gas chimneys in the Makran accretionary prism. Meanwhile, the relationship between the formation and accumulation of NGH and these diapir structures is yet to be revealed. In this paper, the distribution, development and evolution characteristics of the mud diapir, mud volcano, and gas chimney in the Makran accretionary prism were obtained based on comprehensive interpretation of multi-channel seismic data, sub-bottom profile data, and multi-beam topography achieved by R/V "Hai Yang Di Zhi Shi Hao" of Guangzhou Marine Geological Survey during the China-Pakistan joint expedition as well as the seismic data provided by Pakistan. Based on these achievements, the effects of mud diapirs, mud volcanoes, and gas chimneys on NGH were explored, and the mud diapir/gas chimney type hydrate accumulation model and mud volcano type hydrate accumulation model were primarily established. All these aim to provide guidance and references for promoting the exploration of NGH resources in the Makran accretionary prism, offshore Pakistan.

2. Geological setting

The Makran accretionary prism in the North Arabian Sea lies in the offshore area of Pakistan and Iran and is located at the junction of the Eurasian Plate, Arabian Plate, and Indian Plate (Fig. 1). It was formed due to the subduction of the Arabian Plate northward beneath the Eurasian Plate at low speed (about 4 cm/yr) and low angle (<3°) (Harms JC et al., 1984; Demets C et al., 2010). Its offshore part is about 100 km wide (Grando G and McClay K, 2007), with the maximum water depth of about 3500 m. It is distributed in EW trending, with the right-lateral strike-slip Minab fault system as its western boundary and the left-lateral strike-slip Ornach Nal fault system as its eastern boundary (Platt JP et al., 1988; Kukowski N et al., 2001; Grando G and McClay K, 2007). Meanwhile, its southern part is bounded by the extension of the Murray Ridge and the Owen Fracture Zone (Kopp C et al.,

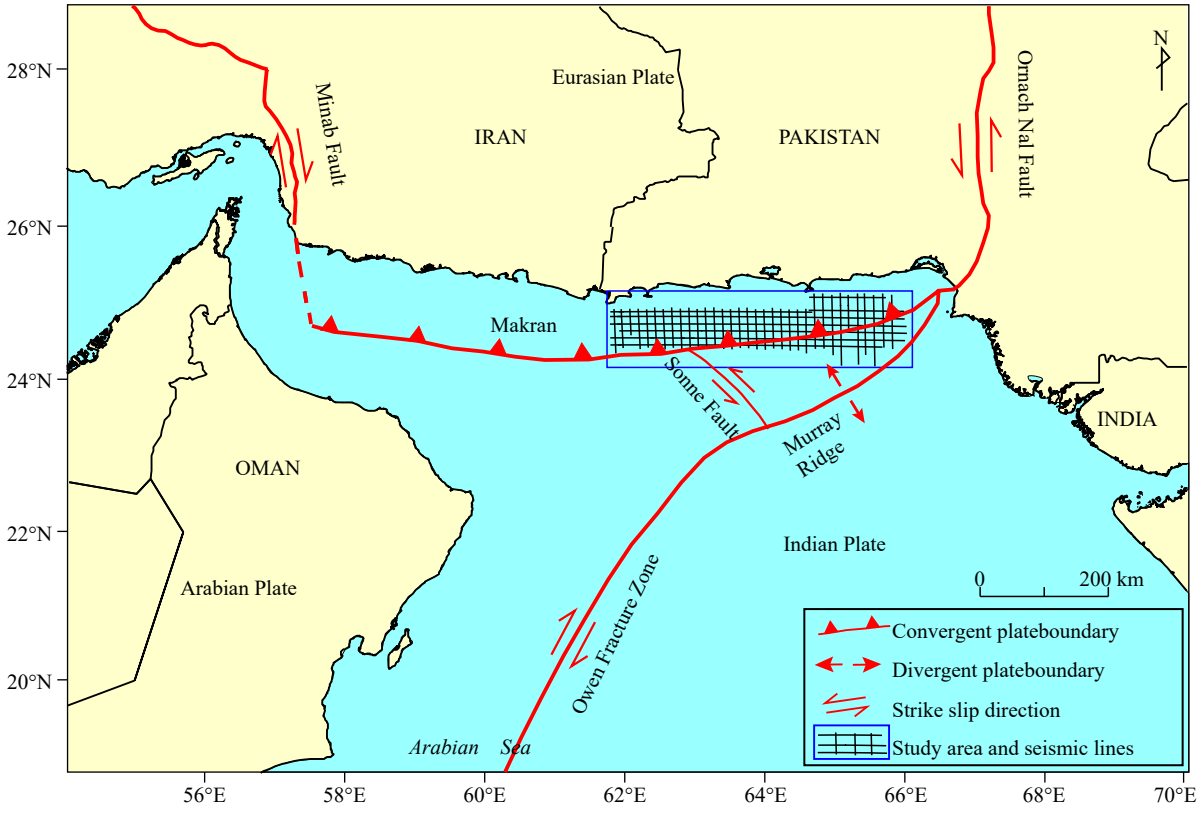

Fig. 1. Tectonic map of the Makran accretionary prism (after Kukowski N et al., 2001).

2000; Fig. 1).

The Makran accretionary prism consists of a narrow continental shelf, a broad continental slope, and a deformation front (Grando G and McClay K, 2007). The slope can be further divided into the upper slope (dips at 7°, width 40 km, water depth 100–1000 m), middle slope (dips at 1°, width 15–20 km, water depth 1000–1500 m), and lower slope (dips at 1°–2°, width 50–60 km, water depth 2000–3000 m) (Gong JM et al., 2018b; Fig. 2a). The lower slope is dominated by simple, imbricate thrust faults that which form seaward verging (Fig. 2b), and the deformation front lies between the lower slope and abyssal plain. The EW thrust faults trend to be increasingly inactive from south to north (Smith G et al., 2012), controlling the development of seven EW anticline ridges, with piggyback basins existing between the ridges (Ellouz N et al., 2007b; Figs. 2a, b).

According to the analysis of onshore stratigraphy and offshore seismic data (Schlüter HU et al., 2002; Gaedicke C et al., 2002; Ellouz N et al., 2007a), the Oligocene, Miocene, Pliocene, and Quaternary strata had been deposited in the offshore area of the Makran accretionary prism since Cenozoic (Fig. 2b), with the thick incoming sediment section of up to 7 km (Kopp C et al., 2000; Grando G and McClay K, 2007). The Oligocene-Middle Miocene strata deposited in deep-water sedimentary environment, showing that the lower part is mainly composed of argillaceous sediments and the upper part consists of sandstones interbedded with mudstones. The Upper Miocene strata share syndepositional development with thrust faults, showing that multiple piggyback depressions are connected through deposition and silty sediments have developed. The Pliocene-Quaternary strata developed typical continental shelf-slope deposits, and are characterized by the development of hemipelagic argillaceous sediments and turbidite sediments (Liao J et al., 2019). The strata in the Makran accretionary prism exhibit density inversion in general, with the lower strata mainly consisting of argillaceous sediments and the upper strata mainly composed of sandy sediments. Meanwhile, the strata had been deposited at a high rate of up to 400 m/Ma since Pliocene (Abid H et al., 2015). These stratigraphic distribution feature lay a good material base for the development of the mud diapirs and mud volcanoes in the Makran accretionary prism.

3. Development and distribution characteristics of diapir structure

Diapir structure are widely developed in the Makran accretionary prism. They are mainly present in the forms of mud diapirs, mud volcanoes, and gas chimneys, whose basic characteristics are described as follows.

3.1. Development and distribution characteristics of mud diapirs

According to the features such as the profile morphology, arching height, and activity energy on the seismic profiles, the

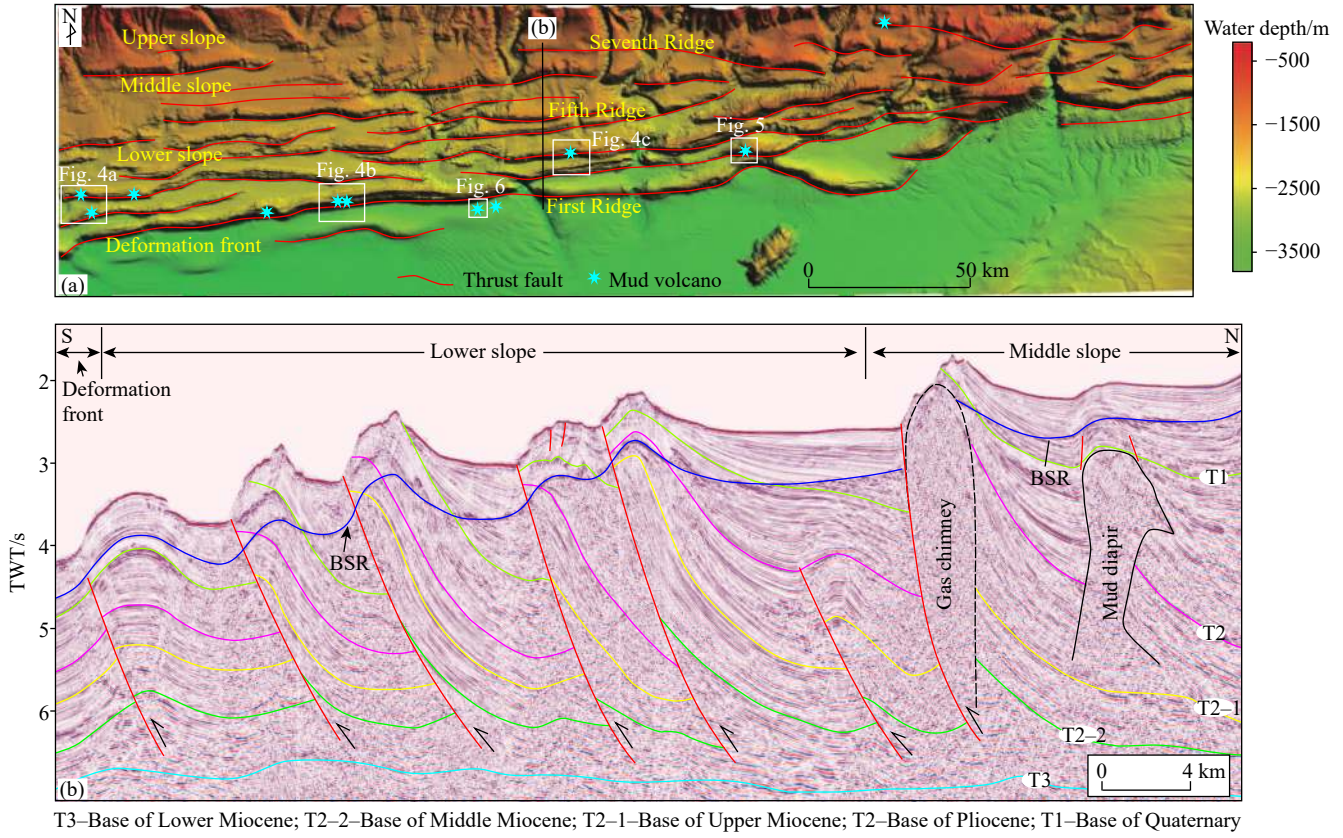

Fig. 2. Structure map (a) of the Makran accretionary prism (thrust fault after Smith G et al., 2012) and imbricate structure of the thrust faults in the Makran accretionary prism (b).

mud diapirs in the Makran accretionary prism can be divided into two types: (1) The ones with low arching amplitude and weak-medium activity energy and, (2) those with high arching amplitude and medium-strong activity energy (Fig. 3).

(i) Mud diapirs with low arching amplitude and weak-medium activity energy. As shown in Fig. 3a, a few of the mud diapirs of this type are distributed in the study area and their main characteristics are as follows. It has a profile morphology featuring a wide lower part and a narrow upper part –similar to a turtle-back anticline (Fig. 3ai). It shows discontinuous chaotic reflection with weak amplitude (Fig. 3aii). It is characterized by low arching amplitude and weak energy of internal activities. The lower part of the mud diapir features a maximum width of 10 km according to seismic profiles. However, it invade upwards at low arching amplitude and only pierce the bottom boundary of Pliocene, leading to the deformation of the overlying strata and the small-scale upward pulling of the strata at both sides. Moreover, there are few accompanied faults near the mud diapirs since they are covered by overlying strata.

(ii) Mud diapirs with high arching amplitude and medium-strong activity energy. As shown in Figs. 2b, 3b, the mud diapirs of this type are widely distributed in the study area. They are mainly developed on middle and upper slopes. Their

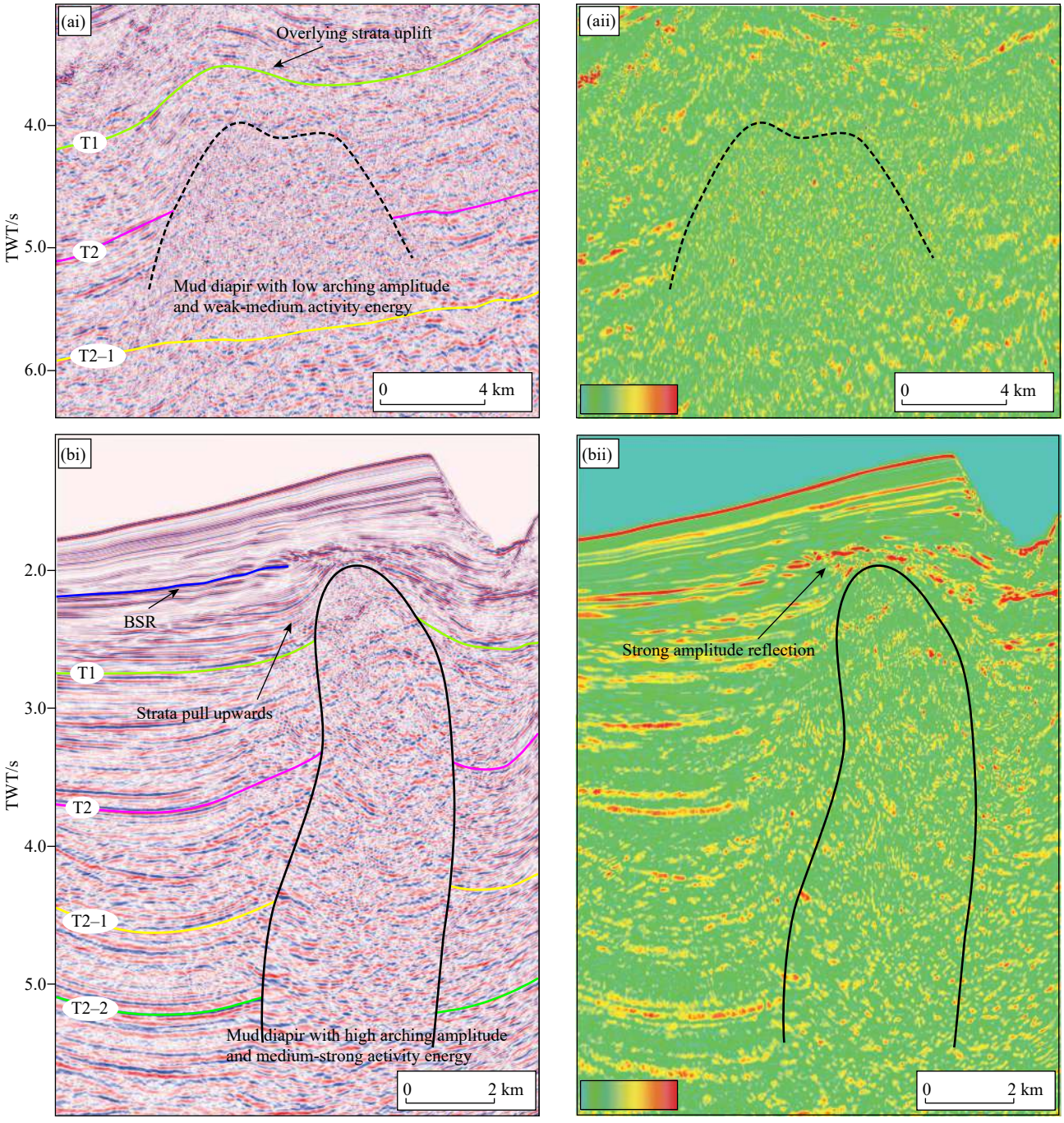

T2–2–Base of Middle Miocene; T2–1–Base of Upper Miocene; T2–Base of Pliocene; T1–Base of Quaternary

Fig. 3. Seismic and instantaneous amplitude profiles of mud diapirs in the Makran accretionary prism.

profiles take a vertically or irregularly columnar morphology and they are in unconformable contact with the surrounding rocks (Fig. 3bi). It shows discontinuous chaotic reflections with weak amplitude inside (Fig. 3bii) and is characterized by high arching amplitude and strong energy of internal activities. It is about 4 km wide according to the seismic profiles. However, it penetrates Middle Miocene –Pliocene strata and pierces the bottom boundary of Quaternary, almost reaching the seafloor. BSRs have developed near the top of the mud diapir, with obvious strong amplitude seismic reflection (Fig. 3bii). The strata on both sides are apparently pulled upwards. Meanwhile, a series of tensional faults have developed in some overlying strata subject to the arcing tension. Pockmarks were observed on the seafloor corresponding to some mud diapir developed areas, which are sags on the seafloor surface caused by decompression during the upward invasion of the mud diapirs.

According to the interpretation of multi-channel seismic data covering more than 5000 km, the characteristics of the mud diapirs in the Makran accretionary prism are summarized. (1) They show different morphologies, vertically columnar, coniform, or irregular. (2) They are distributed increasingly from offshore areas toward onshore areas. They are mainly distributed on the middle slope in the central and western parts and are mainly distributed on the upper slope in the eastern part. (3) They are distributed in different scales, which are small in the western part and tend to increase towards the eastern part. (4) They are distributed increasingly from the west toward the east, which is related to multiple factors such as the convergence rate of plates, the activities of strike-slip faults, and deposition rate.

3.2. Development and distribution characteristics of mud volcanoes

Some of the mud diapirs in the Makran accretionary prism that are accompanied with the thrust faults feature extremely strong energy of internal activities. They are characterized by high arching amplitude and can penetrate the seafloor to form mud volcanoes. As discovered by previous studies, the mud volcanoes in Makran are mainly developed along the anticline ridges of the middle and upper slopes affected by the convergence rate, strike-slip faults, and the location of plate subduction (Platt JP et al., 1985, 1988; Platt JP, 1986). Some of the mud volcanoes are also developed on the lower slope and the deformation front. Since the temperature and pressure of the mud volcanoes on the middle and upper slopes are unfavorable for the formation of NGH, this paper mainly focused on the study of the mud volcanoes on the lower slope and the deformation front.

As identified from the multi-beam topographic map, ten mud volcanoes have developed along the anticline ridges of the lower slope (the ridges of Nos. 1–3) and the deformation front (Fig. 2a). Their outer morphologies vary, with the tops being coniform (Fig. 4a), flat (left of Fig. 4b), collapsed (right of Fig. 4b), nearly hummocky (Figs. 4c, 5), or dome-shaped (Fig. 6). The coniform mud volcanoes have steep wings, while the mud volcanoes of other shapes have gentle wings. All of the mud volcanoes are nearly symmetric despite their various morphologies, with a diameter of 1 –1.7 km and a height of 20 –150 m above the seafloor. Ring-shaped depressions surround the tops of the mud volcanoes, and slump structures occur on seaward sides of some anticline ridges where mud volcanoes located (Fig. 4).

Fig. 5 shows the sub-bottom profile of a mud volcano along the second anticline ridge in the southern part of the lower slope as well as the topographic features, the location of the mud volcano is marked in Fig. 2a. The mud volcano has a hummocky top, with a diameter of about 1.55 km and a height of 80 m. Acoustic blank zone can be observed beneath the mud volcano from the sub-bottom profile, denoting the migration pathways of the materials inside the mud volcano. As shown in the topographic map, ring-shaped depressions surround the mud volcano and slump structures occur on the southern side of the anticline ridge. Wiedicke M et al. (2001) analyzed mud volcanoes on the deformation front based on high-resolution seismic data, including the one as shown in Fig. 6 (its location is marked in Fig. 2a). It is present as a dome-shaped structure on the topographic map, with a diameter of about 1.7 km and a height of about 50 m above normal seafloor. It is present as a coniform structure bulging from the seafloor on the seismic profile, with the reflection blank zones denoting migration pathways, which gradually narrow from bottom to top.

Mud volcanoes are developed along the anticline ridges in the southern part of the lower slope and the deformation front of the Makran accretionary prism for the following reasons. There is provenance coming from the north, and the overlying sediments on the top of the southern anticline ridges and the deformation front are thin, thus causing low pressure. Moreover, the southern thrust faults in the accretionary prism are strongly active. All these are favorable for the high-pressure fluids in deep sources to pierce the seafloor surface to form mud volcanoes.

3.3. Development and distribution characteristics of gas chimneys

The seismic features of the gas chimneys at different tectonic locations in the Makran accretionary prism were analyzed. As a result, three types of typical gas chimneys were identified (Fig. 7), and they are described as follows.

(i) Gas chimneys in piggyback basins. The gas chimneys of this type are located in the piggyback basins between the ridges and are vertically columnar in shape (Fig. 7a). According to the characteristics such as morphology and spatial distribution, a gas chimney of this type can be divided into three parts, namely the root zone, passing area, and apical zone from bottom to top (Fig. 7ai). (1) The root zone serves as the initial part for the development of the gas chimney. It is located in the Middle Miocene and shows the reflection features of weak-medium amplitude, low frequency, and poor

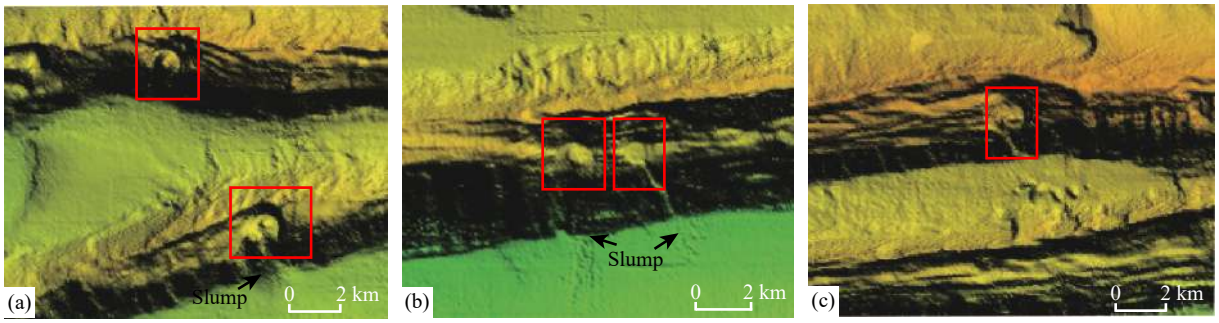

Fig. 4. Topographic characteristics of mud volcanoes on the lower slope (location in Fig. 2a).

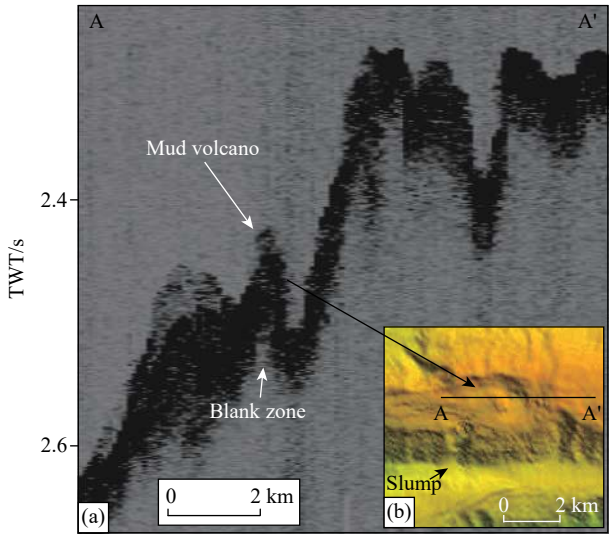

Fig. 5. Sub-bottom profile (a) and submarine topography (b) of mud volcanoes on the lower slope (location in Fig. 2a).

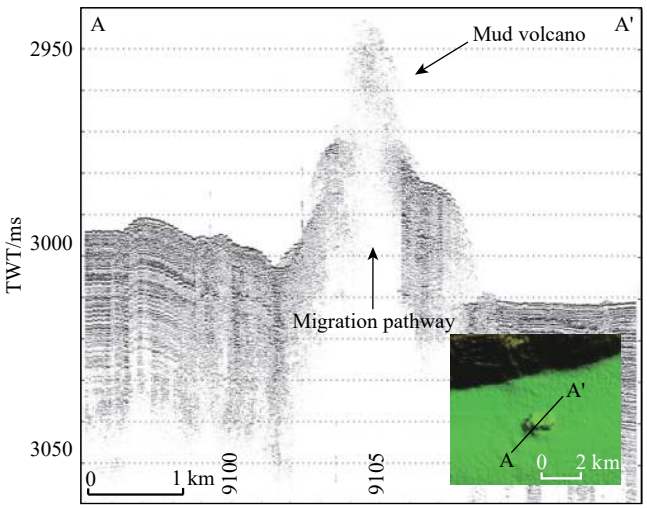

Fig. 6. Characteristics of mud volcanoes on the deformation front (seismic profile after Wiedicke M et al., 2001) (location in Fig. 2a).

continuity on the seismic profile. (2) The passing area is the main part of the gas chimney. It shows the following reflection characteristics on the seismic profile. The seismic event in the lower part feature discontinuity and low frequency, and the internal seismic event are pulled down, attributed to the decrease in shear wave velocity in the strata resulting from the presence of gas-bearing strata. While the middle and upper parts show chaotic reflection. (3) The apical zone extends upwards to the seafloor. It shows a weakened internal amplitude, which is close to blank reflection (Fig. 7aii). BSRs, as well as high-impedance anomalous bodies with locally increased internal amplitude and large wave impedance difference, are developed between the apical zone and the passing area. They are indicated as NGH enriched areas. Furthermore, mound are formed on the seafloor, which is possibly owing to the sediment expansion resulting from NGH formation (Fig. 7ai). Plumes have been observed on the seafloor areas corresponding to the gas chimneys of this type, indicating that the gas migrated upwards, and there are sufficient gas sources.

(ii) Gas chimneys along active anticline ridges. The gas chimneys of this type are located along active anticline ridges. They are accompanied with thrust faults, develop on the hanging wall, and take the shape of nearly vertical column (Figs. 2b, 7b). According to the characteristics such as morphology and spatial distribution, a gas chimney of this type can also be divided into three parts, namely the root zone, passing area, and apical zone from bottom to top (Fig. 7bi). (1) The root zone is located in the Middle Miocene and shows the reflection features of weak amplitude, low frequency, and poor continuity on the seismic profile. (2) The seismic reflection of the passing area is mainly characterized by chaotic reflection, with the enhanced amplitude occurring in local areas of its wings (Fig. 7bii). Furthermore, it is accompanied by bright spots, indicating the migration of gas-bearing fluids. The seismic event in the lower part of the passing area are apparently pulled down, denoting that gas invasion occurred. (3) The apical zone extends upwards to the seafloor. It shows chaotic reflection in general, with some areas exhibiting bright spots with enhanced amplitude, reversed polarity, and decreased frequency (Fig. 7bi), indicating the migration of gas-bearing fluids. In addition, slump structures occurred on the seafloor, pockmarks formed on the top of the anticline ridges, and blank reflection presented beneath the pockmarks (Fig. 7bi). All these indicate that there are NGH in the sedimentary strata and gas leakage may have occurred.

(iii) Gas chimneys along inactive anticline ridges. The gas chimneys of this type are located along the inactive anticline ridges and developed on the hanging wall of the buried

inactive faults (Fig. 7c). The anticline ridges were formed early, the faults are not active any longer and covered by overlying strata. With irregular lower part and large top, the gas chimney of this type take the shape of mushroom (Fig. 7ci). (1) The root zone is developed in the top of the Lower Miocene, showing the reflection features of weak-medium amplitude, medium frequency, and poor continuity. (2) The passing area shows chaotic seismic reflection, with bright spots with enhanced amplitude, reversed polarity, and decreased frequency occurring in the upper part (Fig. 7ci), indicating the presence of gas-bearing strata. Furthermore, the seismic event in the lower part of the passing area are pulled

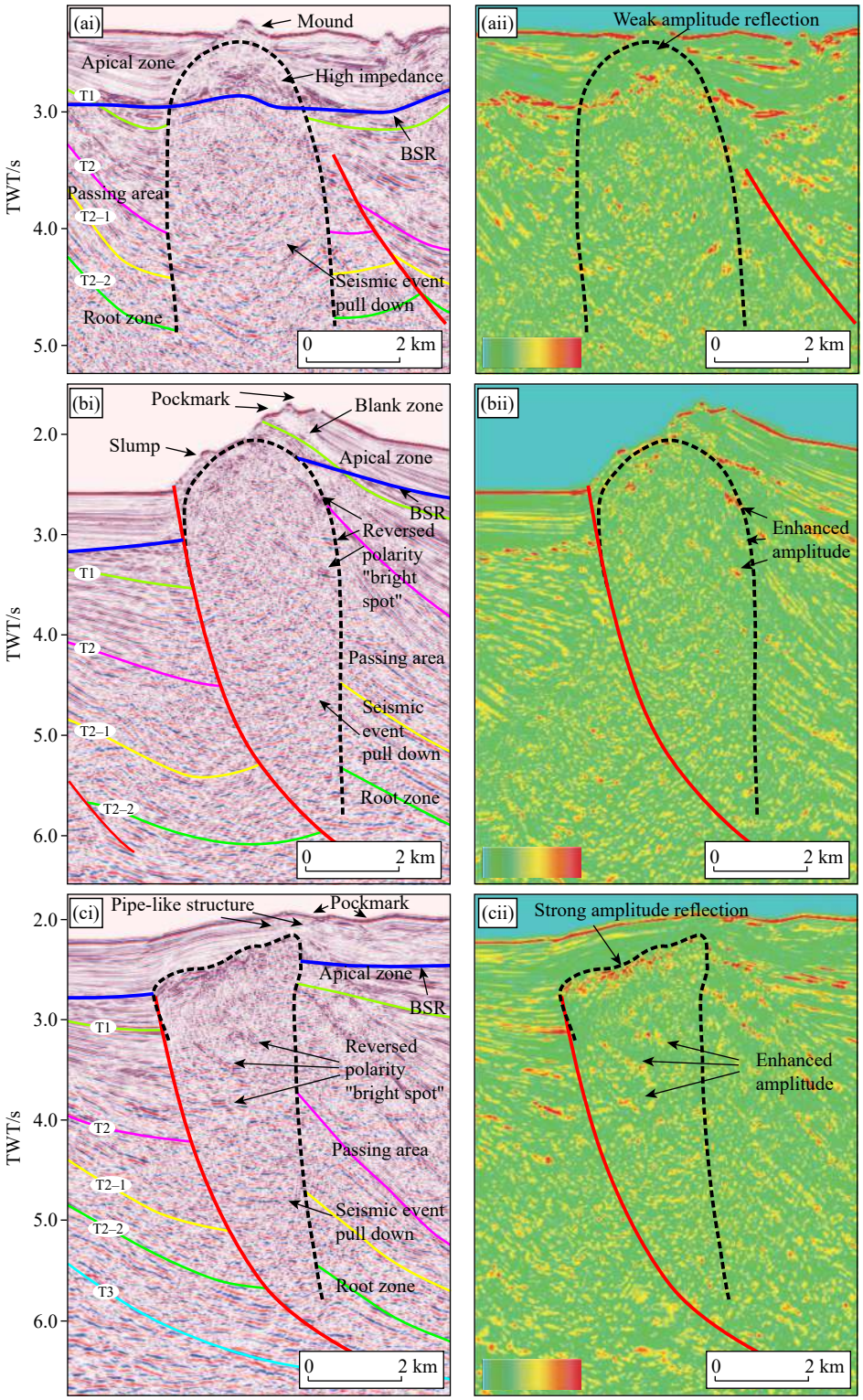

T3–Base of Lower Miocene; T2–2–Base of Middle Miocene; T2–1–Base of Upper Miocene; T2–Base of Pliocene; T1–Base of Quaternary

Fig. 7. Seismic and instantaneous amplitude profiles of gas chimneys in the Makran accretionary prism.

down at smaller amplitude compared to the gas chimneys of the two types mentioned above, which is possibly caused by low gas content in the gas chimneys or gas leakage. (3) The apical zone ends in the Holocene. Its top interface are larger and shows strong amplitude reflection (Fig. 7cii), which is possible caused by gas enrichment in the top and diffuses towards both sides. Pipe-like structures for gas effusion are developed between the top of the gas chimneys and the seafloor (Fig. 7ci), which can serve as the pathways for gas to vertically migrate to the seafloor. Meanwhile, pockmarks are visible on the seafloor corresponding to the gas chimneys, indicating that gas leakage may have occurred.

In summary, the gas chimneys in the Makran accretionary prism mainly have the following characteristics. (1) Their external reflection morphologies are vertically columnar or irregular or coniform. (2) They are mainly distributed on the middle slope in the western and central parts of the accretionary prism and are sparsely distributed in the eastern part, with different scales. (3) Most of them are located along the anticline ridges and are accompanied with thrust faults. (4) They had been active since the Early Miocene, and the gas chimneys at different tectonic locations started to be active at different time and penetrated different horizons. (5) Bright spots shown in the passing areas and the apical zones of the gas chimneys indicate gas in deep sources migrated upwards and gas leakage is still currently active.

4. Effects of diapir structure on gas hydrate accumulation

The Oligocene–Middle Miocene hugely-thick under-compacted argillaceous sediments in deep water serve as the mud sources for the formation of mud diapirs and mud volcanoes. Furthermore, they have hydrocarbon-generating potential, thus assuring that there are sufficient gas sources for the formation of NGH in the Makran accretionary prism. BSRs in the accretionary prism mainly developed in the Pliocene strata and lower part of the Quaternary. The mass-transport deposits and coarse clastic alluvial fans in the strata are favorable for the storage and enrichment of NGH.

As can be seen from the seismic data (Figs. 2b, 3, 7) and planar distribution map (Fig. 8) of the mud diapirs, gas chimneys, bright spots and BSRs spatially agree well with the mud diapirs, gas chimneys and bright spots. In terms of planar distribution, most mud diapirs and gas chimneys have developed in the areas where BSRs distributed, especially in the central and western parts. Vertically, BSRs can be clearly identified on the tops and the peripheries of the mud diapirs (Figs. 2b, 3) as well as in the upper part of gas chimneys and its surrounding areas (Fig. 7) in general. The bright spots with strong amplitude presented on the top of the mud diapirs and gas chimneys, serve as the evidence that there may exist a small amount of residual free gas. All these fully indicate that the formation, distribution, and enrichment of NHGs are caused by and corresponding to the structures such as the mud diapir, mud volcano and gas chimney. As can also be observed from the seismic profile, BSRs are not interrupted when go through the thrust faults and show good continuity (Fig. 2b). Meanwhile, a number of bright spots are shown in the lower slope of the central and western parts of the Makran accretionary prism, indicating the thrust faults also provide good pathways for gas migration. The gas will accumulate in a suitable environment after migrating to shallow strata. In this way, NGH are formed.

Despite featuring few accompanied faults, the mud diapirs with low arching amplitude and weak-medium activity energy still have some micro-fissures and fractures, which serve as the pathways for gas to migrate upwards. The mud diapirs with high arching amplitude and medium-strong activity energy are very favorable for the formation of NGH, since their arching process will usually cause faults and fractures to be formed in the overlying strata and surrounding rocks. The mud diapirs along with the accompanied faults and fractures constitute favorable pathways through which the gas in deep sources migrate upwards to the Gas Hydrate Stability Zone (GHSZ). Meanwhile, the arching process of the mud diapirs will lead to the deformation of the overlying strata, thus changing the local hydrodynamic conditions and creating a suitable environment for fluid drainage (Lee MW et al., 1994; Sha ZB et al., 2005). Furthermore, local thermal effects inducing from the development of mud diapirs provides a good condition for the production of biogenic gas, which serves as a significant gas source for the formation of NGH (Rice DD and Claypool GE, 1981; Luan XW, 2009). The NGH reservoirs in the Makran accretionary prism have mainly developed in Pliocene and Quaternary, which are bathyal-abyssal argillaceous sediments and turbidites sediments. The reservoirs consisting of argillaceous sediments feature poor physical properties. However, the faults and cracks formed inside the mud diapirs and their surrounding rocks during the development of the mud diapirs can effectively improve the porosity and permeability of the strata, thus providing accumulation space for hydrate. In this way, the fracture filling type hydrate can be formed.

As indicated by the hydrate accumulation models and relevant drilling data all through the world (Ginsburg GD et al., 1999; Milkov AV, 2000; Milkov AV and Sassen R, 2002), hydrate tends to form around mud volcanoes owing to rapid cooling of gas during the migration of gas from deep sources towards shallow strata. Therefore, the hydrate in the mud volcanoes are mostly distributed in ring shapes around the mud volcanoes. Wiedicke M et al. (2001) found that the methane concentrations in the sediments from the mud volcanoes and their vicinity on the deformation front are up to 40000 ng/g, indicating sufficient gas sources in the Makran accretionary prism. Plumes were observed in five out of ten mud volcanoes found in the study area. This indicates that the heat flow anomalies resulting from the migration and eruption of the materials inside the mud volcanoes destroyed the GHSZ and led to NGH dissociation. As a result, the methane was released into waters and thus plumes were formed. After the eruption, the thermal effect caused by mud volcanoes disappeared gradually and the temperature and pressure field were restored to the normal levels. Then the methane migrates

to the GHSZ once again through the pathways inside the mud volcanoes and then accumulates around mud volcanoes. The periodic activities consisting of eruption and dormancy of the mud volcanoes cause the hydrate formed to be in a dynamic equilibrium state composed of generation-dissociation-regeneration. The slump structures occur on seaward sides of some anticline ridges where mud volcanoes located can serve as suitable sites for hydrate accumulation, while they may also be formed from the dissociation of gas hydrate (Zhang GX et al., 2006; Kong L et al., 2018; Shi YH et al., 2019). Further research is required to determine the effects of slump structures in various parts of the Makran accretionary prism on hydrate.

Affected by two stages of compression and nappe in Paleocene and Middle Miocene –Pliocene (Platt JP et al., 1988), the fault structures inside the Makran accretionary prism were active. These destroyed the sealing pressure inside the Oligocene–Middle Miocene mudstones and prompted the gas in deep sources to migrate upwards along the faults or the weak tectonic zones subject to super pressure. As a result, the gas chimneys were formed. The root zones of the gas chimneys serve as the initial parts for pressure release of superpressured gas in deep sources. Then the gas migrates upwards along the pathways inside the gas chimneys, during which both pressure and temperature gradually decline and the gas accumulates in the upper parts of the gas chimneys. When the gas saturation reaches a certain level, the bright spots denoting strong amplitude occur on the seismic profile. Normal faults had developed in shallow strata since Late Pliocene (Grando G and McClay K, 2007), and the gas migrates into the GHSZ such as the flanks of gas chimneys or overlying favorable reservoirs in shallow strata through the fault system or by means of seepage. In this way, the hydrate are formed and accumulate, and may lead to the development of mounds on the seafloor (Liu B et al., 2020).

The direct function of the mud diapirs and mud volcanoes as migration pathways is to have provided high-flux methane (Liu J et al., 2015). Plumes are visible on the multiple seafloor areas corresponding to the mud diapirs, mud volcanoes and gas chimneys in the Makran accretionary prism. This indicates that the methane content is very high in these areas and a certain scale of gas effusion has occurred on the seafloor. Fischer D et al. (2013) calculated the depth of SMT (sulphate/methane transition) at two stations near the mud volcanoes on the deformation front, which is 1.3 m and 4.7 m, respectively. The shallow SMT also indicates high methane flux and sufficient gas sources in the Makran accretionary prism. According to comprehensive analysis, the Makran accretionary prism enjoys considerable NGH resources potential. Meanwhile, the surrounding areas of the tops of mud diapirs and mud volcanoes, as well as the upper part of gas chimneys and its surrounding areas, are potential hydrate enrichment areas.

5. Discussion on hydrate accumulation model

A series of imbricate thrust faults, mud diapirs, mud volcanoes, and gas chimneys that are widely developed in the Makran accretionary prism constitute the main pathways for gas migration. They control the formation, accumulation, and distribution of NGH. In the accretionary prism, the mud diapirs are increasingly distributed from offshore areas toward onshore areas. They are mainly distributed on the middle slope in the central and western parts and on the upper slope in the eastern part. The mud diapirs distributed on the middle slope in the central and western parts agree well with BSRs. The mud volcanoes are mainly concentrated along the southern anticline ridges of the lower slope and the deformation front. The gas chimneys are mainly distributed on the middle slope in the central and western parts. Most of them are accompanied with thrust faults or developed in the weak tectonic zones induced by faults, thus providing a good discharge system for the gas in deep parts to migrate upwards.

Based on the aforementioned analysis, the mud diapirs and gas chimneys on the middle slope have significant effects on the formation and accumulation of hydrate, and develop mud diapir/gas chimney type hydrate. Meanwhile, mud volcano type hydrate develop on the south lower slope and the deformation front. Gong JM et al. (2018a) analyzed and concluded that the stepped accretionary prism type hydrate developed in the central and northern parts of the lower slope.

In this paper, the mud diapir/gas chimney type hydrate accumulation model and the mud volcano type hydrate accumulation model in Makran accretionary prism were primarily established. (1) The mud diapir/gas chimney type hydrate accumulation model on the middle slope (Fig. 9a). The mud diapir and gas chimney structures developing along the anticline ridges and the piggyback basins, as well as the faults or tectonic fissures in shallow strata, jointly constitute a good discharge system, which helps gas to migrate from deep sources to the GHSZ, and then NGH are formed. BSRs feature good continuity in the upper parts of the structures and their surrounding areas. Furthermore, in corresponding seafloor areas, pockmark/slump structures may be formed owing to gas leakage or mound may develop due to the sediment expansion resulting from NGH formation. (2) The mud volcano type hydrate accumulation model on the south lower slope and the deformation front (Fig. 9b). As for the mud volcanoes accompanied with active thrust faults along the anticline ridges and the mud volcanoes developing in the comparatively flat deformation front, their internal materials constitute the pathways for the gas to migrate, which is favorable for the gas in deep sources to migrate upwards to shallow strata. Since high-heat flow inside the mud volcanoes has adverse effects on the accumulation of hydrate to some extent, BSRs in the upper parts of the mud volcanoes are “interrupted” by the migration pathways. Therefore, hydrate are mainly distributed around the mud volcanoes. The gas migrates to the seafloor through faults or fissures in shallow strata, and plumes are formed.

As can be seen from the distribution map of mud diapirs, gas chimneys, bright spots, and BSRs in the Makran accretionary prism in Fig. 8, BSRs are widely distributed on the middle slope and lower slope in the central and western

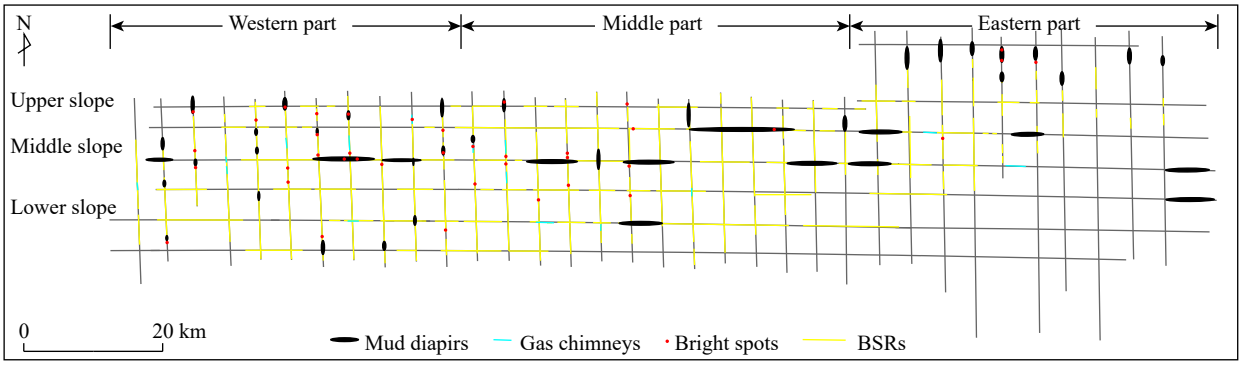

Fig. 8. Distribution map of mud diapirs, gas chimneys, bright spots, and BSRs in the Makran accretionary prism.

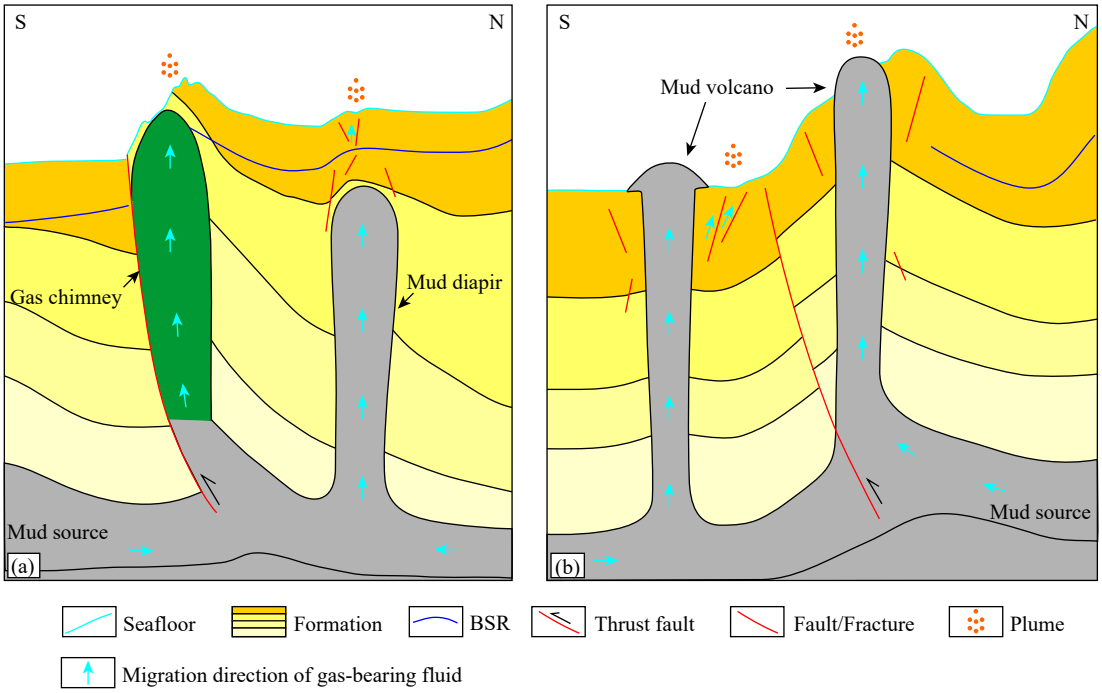

Fig. 9. Sketch map (a) of mud diapir/gas chimney type hydrate accumulation model and sketch map (b) of mud volcano type hydrate accumulation model.

parts. Meanwhile on the middle slope, BSRs comfortably correspond to the mud diapirs, gas chimneys and bright spots. In the central and northern parts of the lower slope, imbricate thrust faults provide favorable tectonic discharge conditions for the formation and accumulation of hydrate. And in the southern part of the lower slope and the deformation front, mud volcanoes have positive effects on the formation and accumulation of hydrate. According to the comprehensive analysis of development and distribution characteristics of the mud diapirs, mud volcanoes, gas chimneys, bright spots, and thrust faults, as well as the distribution of BSRs and plumes [based on internal expedition data and survey data from a German expedition (Bohrmann G et al., 2008)], the middle slope, lower slope, and deformation front in the central and western parts of the Makran accretionary prism are considered to be the prospect area of NGH.

6. Conclusions

(i) Two types of mud diapirs have developed in the Makran accretionary prism, namely the ones with low arching amplitude and weak-medium activity energy and the ones with high arching amplitude and medium-strong activity energy. The mud diapirs increase from offshore areas toward onshore areas, while the ones favorable for the formation of NGH are mainly distributed on the middle slope in the central and western parts of the accretionary prism.

(ii) Ten mud volcanoes that are favorable for the formation of hydrate in the Makran accretionary prism are mainly concentrated along the anticline ridges in the southern part of the lower slope (the ridges of Nos. 1 –3) and the deformation front.

(iii) Three types of gas chimneys have developed in the Makran accretionary prism, which are located in piggyback basins, active anticlines, and inactive anticlines, respectively. They are mainly distributed on the middle slope in the central and western parts of the accretionary prism and are mostly accompanied with thrust faults. The gas chimneys located at different tectonic locations have different development

characteristics and started to be active at different time and pierced different horizons.

(iv) The mud diapirs, mud volcanoes, and gas chimneys and their accompanied thrust faults serve as the main migration pathways of gas, and thus are the important controlling factors for the formation, accumulation, and distribution of NGH in the Makran accretionary prism. The tops and the peripheries of mud diapirs and mud volcanoes, as well as the upper parts of gas chimneys and the areas near the upper parts, are potential hydrate enrichment areas.

(v) The mud diapirs/gas chimneys type hydrate develop on the middle slope, the mud volcanoes type hydrate develop in the southern part of the lower slope and the deformation front, and the stepped accretionary prism type hydrate develop in the central and northern parts of the lower slope. Therefore, the middle slope, lower slope and deformation front in the central and western parts of the Makran accretionary prism jointly constitute the NGH prospect area.

CRediT authorship contribution statement

Zhen Zhang conceived of the presented idea, performed data interpretation and then wrote the main manuscript text. Gao-wen He, Hui-qiang Yao and Xi-guang Deng provided manuscript reviews, and gave critical comments. Miao Yu provided geological data. Wei Huang and Wei Deng offered help and advice on data interpretation. Syed Waseem Haider, Naimatullah Sohoo and Noor Ahmed Kalhoro provided help on language. All authors discussed the results and contributed to the final manuscript.

Declaration of competing interest

The authors declare no conflicts of interests.

Acknowledgment

This research was supported by projects of China Geological Survey (DD20190582, DD20191009), Key Special Project for Introduced Talents Team of Southern Marine Science and Engineering Guangdong Laboratory (Guangzhou) (GML2019ZD0106). The authors thank Guangzhou Marine Geological Survey for their permission to use the data. A great thanks to the crew members and scientists for their excellent work during the China-Pakistan Joint Marine Scientific Expedition.

References

Abid H, Moin RK, Nadeem A, Tahir J. 2015. Mud diapirism induced structuration and implications for the definition and mapping of hydrocarbon traps in Makran accretionary prism, Pakistan. Washington, AAPG/SEG International Conference & Exhibition, 13–16.

Babadi MF, Mehrabi B, Tassi F, Cabassi J, Vaselli O, Shakeri A, Pecchioni E, Venturi S, Zelenski M, Chaplygin I. 2019. Origin of fluids discharged from mud volcanoes in SE Iran. Marine and Petroleum Geology, 106, 190–205. doi: 10.1016/j.marpetgeo.2019.05.005.

Bohrmann G, Bahr A, Brinkmann F, Brüning M, Buhmann S, Diekamp V, Enneking K, Fischer D, Gassner A, von Halem G, Huettich D, Kasten S, Klapp S. 2008. Cold seeps of the Makran subduction zone (continental margin of Pakistan): R/V Meteor cruise report M74/3: M74, Leg 3, Fujairah-Male, 30 October-28 November, 2007. Berichte, Fachbereich Geowissenschaften, Universität Bremen, No. 266, 1–161.

Demets C, Gordon RG, Argus DF. 2010. Geologically current plate motions. Geophysical Journal International, 181(1), 1–80. doi: 10.1111/j.1365-246x.2009.04491.x.

Dong WL, Huang BJ. 2000. Fluid fracturing, thermal fluid activity and episodic migration of natural gas in Yinggehai Basin. Petroleum Exploration and Development, 27(4), 36–40 (in Chinese with English abstract).

Ellouz N, Deville E, MÜller C, Lallemant S, Subhani AB, Tabreez AR. 2007a. Impact of sedimentation on convergent margin tectonics: Example of the Makran accretionary prism (Pakistan)//Lacombe O, Roure F, Lavé J, Vergés J (Eds.). Thrust Belts and Foreland Basins. Springer, France, Chapter 17, 327–350.

Ellouz N, Lallemant S, Castilla R, Mouchot N. 2007b. Offshore frontal part of the Makran accretionary prism: The Chamak survey (Pakistan). Frontiers in Earth Sciences, 18, 351–366. doi: 10.1007/978-3-540-69426-7_18.

Fischer D, Mogollón JM, Strasser M, Pape T, Bohrmann G, Fekete N, Spiess V, Kasten S. 2013. Subduction zone earthquake as potential trigger of submarine hydrocarbon seepage. Nature Geoscience, 6(8), 647–651. doi: 10.1038/ngeo1886.

Gaedicke C, Prexl A, Schlüter HU, Meyer H, Roeser H, Clift P. 2002. Seismic stratigraphy and correlation of major regional unconformities in the northern Arabian Sea. Geological Society London Special Publications, 195(1), 25–36. doi: 10.1144/gsl.sp.2002.195.01.03.

Ginsburg GD, Milkov AV, Soloviev VA, Egorov AV, Cherkashev GA, Vogt PR, Crane K, Lorenson TD, Khutorskoy MD. 1999. Gas hydrate accumulation at the Håkon Mosby Mud Volcano. Geo-Marine Letters, 19(1–2), 57–67. doi: 10.1007/s003670050093.

Gong JM, Liao J, Yin WH, Zhang L, He YJ, Sun ZL, Yang CS, Wang JQ, Huang W, Meng M, Cheng HY. 2018a. Gas hydrate accumulation models of Makran accretionary wedge, northern Indian Ocean. Marine Geology & Quaternary Geology, 38(2), 148–155 (in Chinese with English abstract).

Gong JM, Liao J, Zhang L, He YJ, Zhai B, Meng M, Cheng HY. 2018b. Discussion on the distribution and main controlling factors of mud volcanoes in Makran accretionary wedge, northern Indian Ocean. Geoscience, 32(5), 1025–1030 (in Chinese with English abstract).

Grando G, McClay K. 2007. Morphotectonics domains and structural styles in the Makran accretionary prism, offshore Iran. Sedimentary Geology, 196(1), 157–179. doi: 10.1016/j.sedgeo.2006.05.030.

Gutscher MA, Westbrook GK. 2009. Great earthquakes in slow-subduction, low-taper margins. In: Lallemand S, Funiciello F (Eds.). Subduction Zone Geodynamics. Berlin, Springer-Verlag Berlin, 119–133.

Harms JC, Cappel HN, Francis DC. 1984. The Makran Coast of Pakistan; its stratigraphy and hydrocarbon potential. In: Haq BU, Milliman JD (Eds.). Marine Geology and Oceanography of Arabian Sea and Coastal Pakistan. Van Nostrand Reinhold, New York, 3–26.

He JX, Huang HY, Chen LC. 1994. The formation and evolution of mud diapir and its relationship with hydrocarbon accumulation mechanism in Yinggehai Basin. Acta Sedimentologica Sinica, 12(3), 120–129 (in Chinese with English abstract).

He JX, Wan ZF, Zhang W, Yao YJ, Su PB, Xu X. 2019. Development and evolution of mud diapir/mud volcano and their relationship with accumulation of petroleum and natural gas hydrate in northern South China Sea. Beijing, Science Press, 1–2 (in Chinese).

Kong L, Zhang ZF, Yuan QM, Liang QY, Shi YH, Lin JQ. 2018. Multi-factor sensitivity analysis on the stability of submarine hydrate-bearing slope. China Geology, 1, 367–373. doi: 10.31035/cg2018051.

Kopp C, Fruehn J, Flueh ER, Reichert C, Kukowski N, Bialas J, Klaeschen D. 2000. Structure of the Makran subduction zone from wide-angle and reflection seismic data. Tectonophysics, 329(1), 171–191. doi: 10.1016/S0040-1951(00)00195-5.

Kukowski N, Schillhorn T, Huhn K, von Rad U, Husen S, Flueh ER. 2001. Morphotectonics and mechanics of the central Makran accretionary wedge off Pakistan. Marine Geology, 173, 1–19. doi: 10.1016/S0025-3227(00)00167-5.

Lee MW, Hutchinson DR, Agena WF, Dillon WP, Miller JJ, Swift BA. 1994. Seismic character of gas hydrates on the southeastern US continental margin. Marine Geophysical Researches, 16, 163–184. doi: 10.1007/BF01237512.

Liao J, Gong JM, He YJ, Yue BJ, Meng M. 2019. Stratigraphic sequence and developmental process of Makran accretionary prism. Marine Geology Frontiers, 35(4), 69–72.

Liu B, Chen JX, Haider SW, Deng XG, Yang L, Duan ML. 2020. New high-resolution 2D seismic imaging of fluid escape structures in the Makran subduction zone, Arabian Sea. China Geology, 3, 269–282. doi: 10.31035/cg2020027.

Liu J, Sun MJ, Su M, Yang R, Wu NY. 2015. Influence of submarine mud diapirs (mud volcanoes) on gas hydrate accumulation. Geological Science and Technology Information, 34(5), 98–104 (in Chinese with English abstract).

Luan XW. 2009. Sulfate-methane interface: The upper boundary of gas hydrate zone. Marine Geology & Quaternary Geology, 38(2), 148–155 (in Chinese with English abstract).

Milkov AV. 2000. Worldwide distribution of submarine mud volcanoes and associated gas hydrates. Marine Geology, 167(1), 29–42. doi: 10.1016/S0025-3227(00)00022-0.

Milkov AV, Sassen R. 2002. Economic geology of offshore gas hydrate accumulations and provinces. Marine and Petroleum Geology, 19(1), 1–11. doi: 10.1016/S0264-8172(01)00047-2.

Minshull TA, White R. 1989. Sediment compaction and fluid migration in the Makran accretionary prism. Journal of Geophysics Research, 94, 7387–7402. doi: 10.1029/JB094iB06p07387.

Platt JP. 1986. Dynamics of orogenic wedges and the uplift of high-pressure metamorphic rocks. Geological Society of America Bulletin, 97, 1037–1053. doi: 10.1130/0016-7606(1986)972.0.CO;2.

Platt JP, Leggett JK, Alam S. 1988. Slip vectors and fault mechanics in the Makran accretionary wedge, Southwest Pakistan. Journal of Geophysical Research, 93(7), 7955–7973. doi: 10.1029/JB093iB07p07955.

Platt JP, Leggett JK, Young J, Raza H, Alam S. 1985. Large-Scale sediment underplating in the Makran accretionary prism, southwest Pakistan. Geology, 13(7), 507–511. doi: 10.1130/0091-7613(1985)13<507:LSUITM>2.0.CO;2.

Rice DD, Claypool GE. 1981. Generation, accumulation, and resource potential of biogenic gas. AAPG Bulletin, 65(1), 5–25. doi: 10.1306/2F919765-16CE-11D7-8645000102C1865D.

Römer M, Sahling H, Pape T, Bohrmann G, Spieß V. 2012. Quantification of gas bubble emissions from submarine hydrocarbon seeps at the Makran continental margin (offshore Pakistan). Journal of Geophysical Research, 117(C10015), 1–19. doi: 10.1029/2011JC007424.

Schlüter HU, Prexl A, Gaedicke C, Roeser H, Reichert C, Meyer H, von Daniels C. 2002. The Makran accretionary wedge; sediment thicknesses and ages and the origin of mud volcanoes. Marine Geology, 185, 219–232. doi: 10.1016/S0025-3227(02)00192-5.

Sha ZB, Wang HB, Zhang GX, Yang MZ, Liang JQ. 2005. The relationship between diapir structure and gas hydrate mineralization. Earth Science Frontiers, 12(3), 283–288 (in Chinese with English abstract).

Shi WZ, Song ZF, Wang XL, Kong M. 2009. Diapir structure and its origin in the Baiyun depression, Pearl River Mouth Basin, China. Earth Science-Journal of China University of Geosciences, 34(5), 778–784 (in Chinese with English abstract). doi: 10.3799/dqkx.2009.086.

Shi YH, Liang QY, Yang JP, Yuan QM, Wu XM, Kong L. 2019. Stability analysis of submarine slopes in the area of the test production of gas hydrate in the South China Sea. China Geology, 2, 276–286. doi: 10.31035/cg2018122.

Smith G, McNeill L, Henstock TJ, Bull J. 2012. The structure and fault activity of the Makran accretionary prism. Journal of Geophysical Research, 117, 1–17. doi: 10.1029/2012JB009312.

von Rad U, Berner U, Delisle G, Doose-Rolinski H, Fechner N, Linke P, Lückge A, Roeser HA, Schmaljohann R, Wiedicke M, Sonne 122/130 Scientific Parties. 2000. Gas and fluid venting at the Makran accretionary wedge off Pakistan. Geo-Marine Letters, 20(1), 10–19. doi: 10.1007/s003670000033.

Wiedicke M, Neben S, Spiess V. 2001. Mud volcanoes at the front of the Makran accretionary complex, Pakistan. Marine Geology, 172, 57–73. doi: 10.1016/S0025-3227(00)00127-4.

Zhang GX, Zhu YH, Liang JQ, Wu SG, Yang MZ, Sha ZB. 2006. Tectonic controls on gas hydrate deposits and their characteristics. Geoscience, 20(4), 605–612 (in Chinese with English abstract).